

Listen to Interpret: Post-hoc Interpretability for Audio Networks with NMF

Jayneel Parekh, Sanjeel Parekh, Pavlo Mozharovskyi, Florence d’Alché-Buc, and Gaël Richard
LTCI, Télécom Paris, Institut Polytechnique de Paris, France

Abstract. This paper tackles *post-hoc* interpretability for audio processing networks. Our goal is to interpret decisions of a network in terms of high-level audio objects that are also listenable for the end-user. To this end, we propose a novel interpreter design that incorporates non-negative matrix factorization (NMF). In particular, a carefully regularized interpreter module is trained to take hidden layer representations of the targeted network as input and produce time activations of pre-learnt NMF components as intermediate outputs. Our methodology allows us to generate intuitive audio-based interpretations that explicitly enhance parts of the input signal most relevant for a network’s decision. We demonstrate our method’s applicability on popular benchmarks, including a real-world multi-label classification task.

1 Introduction

Deep learning models, while state-of-the-art for several tasks in domains such as computer vision, natural language processing and audio, are typically not interpretable. Their increasing use, especially in decision-critical domains, necessitates interpreting their decisions. A good interpretation is often characterized by its understandability for the end users (see for instance (Gilpin et al., 2018)). More importantly, attributes that aid understandability may largely be dependent on the data modality. In this paper, our aim is to generate *post-hoc* human-understandable interpretations for deep networks that process the audio modality. Here, *post-hoc* interpretability refers to the problem of interpreting decisions of a fixed pre-trained network.

Traditional approaches generate interpretations through input attribution, either directly on the raw input features or on a given simplified representation (Montavon et al., 2018; Selvaraju et al., 2017; Ribeiro et al., 2016; Lundberg & Lee, 2017). To generate more understandable interpretations, a small number of approaches consider other means, such as logical rules (Ribeiro et al., 2018), sentences (Hendricks et al., 2016) and high-level concepts (Ghorbani et al., 2019).

Most existing *post-hoc* interpretability methods are primarily designed for application to images and tabular data. This limits their applicability to other data modalities such as audio. Although many audio processing networks operate on spectrogram-like representations, which can be seen as 2D time-frequency images, a visualization or attribution in this space is not as meaningful to a common user as it is for images (Liberman et al., 1968).

This leads us to build an interpretation system that takes into account audio-specific understandability features. We motivate these features through an example: suppose an audio event detection network deployed in a house recognizes an “alarm” sound event. An ideal interpreter for this classification decision would have the ability to “show” that it was indeed an alarm sound that triggered this decision. To do so, it must be able to localize the alarm amid other events in the house (for *e.g.* dog barks, baby cries, background noise *etc.*) and make it listenable for the end-user. It is important to highlight here the role of listenable interpretations for better understanding of an audio network’s decisions – note that it would be much less meaningful for a human to see the alarm sound as highlighted parts of a spectrogram. Thus making the following aspects important for our system design: (i) generating interpretations in terms of high-level audio objects that constitute a scene, (ii) segmenting parts of the input signal most relevant for a decision and providing it as listenable audio.

To this end, we propose a novel *post-hoc* interpreter for audio that employs a popular signal decomposition technique called Non-negative Matrix Factorization (NMF; Lee & Seung (2001)). NMF seeks to decompose an audio signal into constituent spectral patterns and their temporal activations. Unlike principal component analysis, NMF is known to provide part-based decompositions (Févotte et al., 2018). Owing to these properties, we first use NMF to pre-learn a spectral pattern

dictionary on our training data. This dictionary is then incorporated as a fixed decoder within our interpretation module. Specifically, we train our system to determine an intermediate encoding that performs two roles: (i) is able to reconstruct the input through the fixed NMF dictionary decoder, thus corresponding to time activations for dictionary components, (ii) at the same time, a function of this encoding is able to mimic the classifier’s output. Training with these constraints allows us to generate, for any classifier decision, importance values over spectral patterns in our dictionary. Listenable interpretations are readily produced by inverting most important NMF spectral patterns back to the time domain.

In summary, we make the following contributions:

- We propose a novel NMF-based interpreter module for *post-hoc* interpretability that generates interpretations in terms of meaningful high-level audio objects, listenable for the end-user.
- We present an original formulation that constrains the interpreter encoding through two loss functions, one for input reconstruction through NMF dictionary and the other for fidelity to the network’s decision. From a learning perspective, we show a new way to link NMF with deep neural networks, especially for generating interpretations.
- We extensively evaluate on two popular audio event analysis benchmarks, tackling both multi-class and multi-label classification tasks. The dataset for the latter is very challenging due to its collection in noisy real-world setting. Our method’s design allows us to simulate feature removal and perform *faithfulness* evaluation.

2 Related Works

In this section, we position our work in relation to: (i) interpretability methods for audio, (ii) methods for concept-based interpretability and, (iii) use of NMF within the audio community, in particular, attempts to link it with deep networks.

2.1 Interpretability methods for audio

Some approaches (Becker et al., 2018; Won et al., 2019) have shown usability of attention/visualization techniques for interpreting audio processing networks. However, we focus here more on methods that attempt to address audio interpretability beyond image-based visualizations. A few works have applied the popular LIME algorithm with a simplified input representation more suited for audio. In particular, SLIME (Mishra et al., 2017, 2020) proposes to segment the input along time or frequency. The input is perturbed by switching “on/off” the individual segments. AudioLIME (Haunschmid et al., 2020; Chowdhury et al., 2021) proposes to separate input using predefined sources to create the simplified representation. AudioLIME arguably generates more meaningful interpretations than SLIME as it relies on audio objects readily listenable for end-user. However, it can only be applied for limited applications as it requires existence of known and meaningful predefined sources that compose the input audio. APNet (Zinemanas et al., 2021) takes another promising direction by extending interpretable prototypical networks for audio input. However, this work attempts to build interpretable systems *by-design*. It does not tackle the problem of *post-hoc* interpretation.

2.2 Concept-based interpretability

Our method relies on high-level objects for interpretation. In this sense, it is most closely related to *post-hoc* concept-based methods (Kim et al., 2017; Ghorbani et al., 2019). Approaches based on TCAV (Kim et al., 2017), such as ACE (Ghorbani et al., 2019), ConceptSHAP (Yeh et al., 2019), define concept using a set of images and learn a representation for it in terms of hidden layers of the network, termed as concept activation vector (CAV). Another approach, as opted in *post-hoc* version of FLINT (Parekh et al., 2021), represents concepts by a dictionary of attribute functions over input space. These functions are learnt from the hidden layers of the network and visualized using activation maximization (Mahendran & Vedaldi, 2016), a popular technique in computer vision. These designs for concepts or high-level objects are however neither related to our design, nor suitable for generating interpretations for audio processing networks. This is because they heavily focus on deriving meaning of the concept or attribute functions through images, which is not well understandable for an end-user.

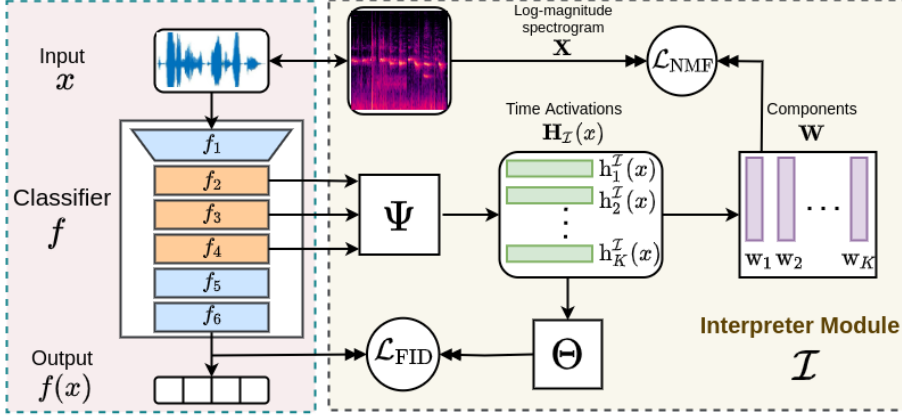


Fig. 1: **System overview:** The interpretation module (right block) accesses hidden layer outputs of the network being interpreted (left block). These are used to predict an intermediate encoding. Through regularization terms, we encourage this encoding to both mimic the classifier’s output and also serve as the time activations of a pre-learnt NMF dictionary.

2.3 NMF for audio

NMF has been widely used within the audio community for numerous tasks ranging from separation to transcription. Its traditional usage as a supervised dictionary or feature learning method involves learning class-wise dictionaries over training data (Févotte et al., 2018). Time activations, which are the so-called features, are generated for any data point by projecting it onto the learnt dictionaries. Extracted features can subsequently be used for downstream tasks such as classification. Work of Bisot et al. (2017) couples NMF-based features with neural networks to boost performance of acoustic scene classification.

NMF has also been successfully employed with audio-visual deep learning models for separation (Gao et al., 2018) and classification (Parekh et al., 2019). Another line of research explored unfolding iterations of different NMF optimization algorithms as a deep neural network (Le Roux et al., 2015a; Wisdom et al., 2017). These systems, commonly known as Deep NMF, have primarily been used for audio source separation tasks.

While these works share with us the idea of combining neural networks and NMF, there is no overlap between our goals and methodologies. Unlike aforementioned studies, we wish to investigate a classifier’s decision in a post-hoc manner using NMF as a regularizer. Furthermore, to our best knowledge, attempting to regress temporal activations of a fixed NMF dictionary by accessing intermediate layers of an audio classification network is novel even within the NMF literature.

3 System Design

An overview of the proposed system is presented in Fig. 1. Our goal is to interpret decisions of a deep classifier f for an input x . In line with concept-based interpretability, we propose to do so through high-level audio patterns. Specifically, outputs of several hidden layers of the classifier are accessed and input to an interpretation module. This module is designed with the aim of mimicking the output of the classifier while satisfying multiple constraints on its intermediate representation, such that it corresponds to our high-level audio pattern activations. We use NMF in two ways for the functioning of our system: (i) to pre-learn a dictionary of spectral patterns over the training data, (ii) use this pre-learnt dictionary as an autoencoding regularizer for our interpretation module. This enforces its intermediate encoding to correspond to NMF component time activations. We detail each of these steps below after a short note on data notation and NMF.

Data notation. We denote a training dataset by $\mathcal{S} := (x, y)_{i=1}^N$, where x is the time domain audio signal and y , a label vector. The label vector could be a one-hot or binary encoding depending upon a multi-class or multi-label dataset, respectively. Since multiple audio representations are used in this paper, a note on their notation is in order. Very often, audio signals are processed in the frequency domain through a short-time Fourier transform (STFT) on x called spectrogram. Log-mel

spectrograms are a popular input to audio classification networks (Peeters & Richard, 2021), which is also the one we use in this paper. Please note that to keep notation simple, we refer to input of the network with x . For NMF however, we favor a representation that can be easily inverted back to the time-domain. In practice, we use a log-magnitude spectrogram \mathbf{X} that is computed by applying an element-wise transformation $x_0 \rightarrow \log(1 + x_0)$ on the magnitude spectrogram. This is preferred over using magnitude spectrograms as it corresponds more closely to human perception of sound intensity (Goldstein, 1967).

NMF basics. NMF is a popular technique for unsupervised decomposition of audio signals (Badeau & Virtanen, 2018). Given any positive time-frequency representation $\mathbf{X} \in \mathbb{R}_+^{F \times T}$ consisting of F frequency bins and T time frames, NMF can be used to decompose it into a product of two non-negative matrices, such that,

$$\mathbf{X} \approx \mathbf{W}\mathbf{H}$$

Here, $\mathbf{W} = [\mathbf{w}_1, \mathbf{w}_2, \dots, \mathbf{w}_K] \in \mathbb{R}_+^{F \times K}$ is interpreted as the spectral pattern or dictionary matrix containing K components and $\mathbf{H} = [\mathbf{h}_1, \mathbf{h}_2, \dots, \mathbf{h}_K]^\top \in \mathbb{R}_+^{K \times T}$ a matrix containing the corresponding time activations. Typically, a β -divergence measure between \mathbf{X} and $\mathbf{W}\mathbf{H}$ is minimized and multiplicative updates are used for estimating \mathbf{W} and \mathbf{H} (Lee & Seung, 2001). Note that it is possible to reconstruct signal corresponding to each or a group of spectral components. This is typically done using a procedure called soft-masking. For a single component k , this is written as,

$$\mathbf{X}_k = \frac{\mathbf{w}_k \mathbf{h}_k}{\mathbf{W}\mathbf{H}} \odot \mathbf{X}$$

Both $./$ and \odot are element-wise operations. If \mathbf{X} is an invertible representation of the magnitude spectrogram, time domain signal for \mathbf{X}_k is easily recovered using the inverse STFT operation. We extensively utilize this procedure for generating listenable interpretations.

NMF can also be used for dictionary learning, by estimating \mathbf{W} on a training dataset matrix $\mathbf{X}_{\text{train}}$. As discussed later, we use a variant of NMF called Sparse-NMF (Le Roux et al., 2015b) to pre-learn dictionary for subsequent usage in the interpretation module.

3.1 Interpreter Design

As depicted in Fig. 1, the interpreter module \mathcal{I} contains three primary blocks: (i) Ψ , which is responsible for generating an intermediate encoding from hidden layer representations of the classification network, (ii) Θ , which attempts to mimic classification network's output given the intermediate representation and, (iii) an NMF dictionary decoder which constrains the intermediate representation to correspond to time activations of a pre-learnt spectral pattern dictionary. To the best of our knowledge, this is an original usage of NMF that allows us to interpret a network's decisions in terms of a fixed dictionary. By design, also enabling us to generate listenable interpretations. Both Ψ and Θ are trained together using gradient based optimization. We discuss below designs for each of the three blocks.

Design of Ψ . The function Ψ processes outputs of a set of hidden layers of the classifier, given by $f_{\mathcal{I}}(x)$. Its output, $\Psi(f_{\mathcal{I}}(x)) \in \mathbb{R}_+^{K \times T}$ produces an intermediate encoding of the interpreter. For simplicity of notation, we will denote this intermediate encoding as $\mathbf{H}_{\mathcal{I}}(x) = \Psi \circ f_{\mathcal{I}}(x)$, a function over input x .

In practice, Ψ is modelled as a neural network that takes as input convolutional feature maps from different layers of f . To concatenate and perform joint processing on them, each feature map is first appropriately transformed to ensure same width and height dimensions. Two important aspects were kept in mind while designing subsequent layers of Ψ . Firstly, audio feature maps for spectrogram-like inputs naturally contain the notion of time and frequency along the width and height dimensions. Secondly, through appropriate regularization we wish to produce an intermediate encoding that also serves as time activations of the pre-learnt NMF dictionary, a matrix of dimensions $K \times T$. To achieve this, we continuously downsample on the frequency axis and upsample the time axis to T frames. Similarly, the number of input feature maps is re-sampled to reach a size of K , equal to the number of components in dictionary \mathbf{W} . All learnable parameters of Ψ are denoted by V_{Ψ} .

Design of Θ . $\mathbf{H}_{\mathcal{I}}(x)$, the intermediate encoding output by Ψ is then fed to Θ , which aims to mimic output of the classifier. This directly helps in learning a representation which can interpret $f(x)$. Its design consists of two parts. The first part pools activations $\mathbf{H}_{\mathcal{I}}(x)$ across time. While

this pooling can be implemented in multiple ways, we opt for attention-based pooling (Ilse et al., 2018), *i.e.*, $\mathbf{z} = \sum_{t=1}^T \mathbf{H}_{\mathcal{I}}(x) \mathbf{a}$, where $\mathbf{a} \in \mathbb{R}^T$ are the attention weights and \mathbf{z} is the pooled vector of dimension $K \times 1$.

The pooled representation vector is passed through a linear layer. This is followed by an appropriate activation function to convert its output to probabilities, that is, softmax for multi-class classification and sigmoid for multi-label classification. All learnable parameters of Θ are denoted by V_{Θ} .

Generalized cross-entropy between interpreter's output $\Theta(\mathbf{H}_{\mathcal{I}}(x))$ and classifier's output $f(x)$ is minimized to encourage interpreter to mimic the classifier. For multi-class classification this loss function is written as,

$$\mathcal{L}_{\text{FID}}(x, V_{\Psi}, V_{\Theta}) = -f(x)^{\top} \log(\Theta(\mathbf{H}_{\mathcal{I}}(x))) \quad (1)$$

On the other hand, for multi-label classification this loss reads,

$$\begin{aligned} \mathcal{L}_{\text{FID}}(x, V_{\Psi}, V_{\Theta}) = & - \sum f(x) \odot \log(\Theta(\mathbf{H}_{\mathcal{I}}(x))) \\ & + (1 - f(x)) \odot \log(1 - \Theta(\mathbf{H}_{\mathcal{I}}(x))). \end{aligned} \quad (2)$$

Here \odot denotes element-wise multiplication.

NMF dictionary decoder. We additionally constrain the intermediate encoding, such that, when fed to a decoder it is able to reconstruct the input audio. As already discussed, we choose this decoder to be a pre-learnt NMF dictionary, \mathbf{W} . Formally, through \mathcal{L}_{NMF} we require $\mathbf{H}_{\mathcal{I}}(x)$ to approximate log-magnitude spectrogram of input audio as $\mathbf{X} \approx \mathbf{W}\mathbf{H}_{\mathcal{I}}(x)$:

$$\mathcal{L}_{\text{NMF}}(x, \mathbf{X}, V_{\Psi}) = \|\mathbf{X} - \mathbf{W}\mathbf{H}_{\mathcal{I}}(x)\|_2^2. \quad (3)$$

This allows us to consider $\mathbf{H}_{\mathcal{I}}(x)$ as a time activation matrix for \mathbf{W} .

Training loss. In addition to \mathcal{L}_{FID} and \mathcal{L}_{NMF} , we impose ℓ_1 regularization on $\mathbf{H}_{\mathcal{I}}(x)$ to encourage sparsity. The complete training loss function over our training dataset \mathcal{S} can thus be given as:

$$\mathcal{L} = \sum_{x \in \mathcal{S}} \mathcal{L}_{\text{FID}} + \alpha \mathcal{L}_{\text{NMF}} + \beta \|\mathbf{H}_{\mathcal{I}}(x)\|_1 \quad (4)$$

where $\alpha, \beta \geq 0$ are loss hyperparameters. All the parameters of the system are constituted in the functions Ψ, Θ and dictionary \mathbf{W} . Since \mathbf{W} is pre-learnt and fixed, the training loss \mathcal{L} is optimized only w.r.t V_{Ψ}, V_{Θ} . As a reminder, when training the interpreter for post-hoc analysis, the classifier network is kept fixed.

Algorithm 1 Learning algorithm

- 1: **Input:** Classifier f , Training data \mathcal{S} , parameters $V = \{V_{\Psi}, V_{\Theta}\}$, hyperparameters $\{\alpha, \beta, \mu\}$, number of batches B , number of training epochs N_{epoch}
- 2: $\mathbf{W} \leftarrow \text{PRE-LEARN NMF DICTIONARY } (\mathcal{S}, \mu)$ { // Sparse-NMF formulation Eq. 5 }
- 3: Random initialization of parameters V_0
- 4: $\hat{V} \leftarrow \text{TRAIN } (f, \mathcal{S}, \mathbf{W}, V_0, \alpha, \beta, B, N_{\text{epoch}})$ { // Train with \mathcal{L} in Eq. 4 }
- 5: **Output:** $\hat{V} = \{\hat{V}_{\Psi}, \hat{V}_{\Theta}\}$

Learning algorithm. The complete learning pipeline is presented in Algorithm 1. The learnable parameters of the interpreter module are given by $V = \{V_{\Psi}, V_{\Theta}\}$.

As for the pre-specified dictionary (Step 2 in Algorithm 1), it is learnt using Sparse-NMF (Le Roux et al., 2015b). Specifically, the following optimization problem is solved through multiplicative updates to pre-learn \mathbf{W} :

$$\begin{aligned} \text{minimize} \quad & D(\mathbf{X}_{\text{train}} | \mathbf{W}\mathbf{H}) + \mu \|\mathbf{H}\|_1 \\ \text{subject to} \quad & \mathbf{W} \geq 0, \mathbf{H} \geq 0, \\ & \|\mathbf{w}_k\| = 1, \forall k. \end{aligned} \quad (5)$$

Training audio files are converted into log-magnitude spectrogram space for factorization. Here $D(\cdot, \cdot)$ is a divergence cost function. In practice, euclidean distance is used. Note that we construct $\mathbf{X}_{\text{train}}$ differently for each of our datasets. The reader is referred to Appendix A.1.1 for more details regarding this construction.

3.2 Interpretation generation

Finally, to generate audio that interprets the classifier’s decision for a sample x and a predicted class c , we follow a two-step procedure:

- The first step consists of selecting the components which are considered “important” for the prediction. This is determined by estimating their relevance using the pooled time activations in Θ and the weights for linear layer, and then thresholding it. Precisely, given a sample x , the pooled activations are computed as $\mathbf{z} = \sum_{t=1}^T \mathbf{H}_{\mathcal{I}}(x) \mathbf{a}$. Denoting the weights for class c in the linear layer as θ_c^w , the relevance of component k is estimated as $r_{k,c,x} = \frac{(\mathbf{z}_k \theta_{c,k}^w)}{\max_l |\mathbf{z}_l \theta_{c,l}^w|}$. This is essentially the normalized contribution of component k in the output logit for class c . Given a threshold τ , the selected set of components are computed as $L_{c,x} = \{k : r_{l,c,x} > \tau\}$.
- The second step consists of estimating a time domain signal for each relevant component $k \in L_{c,x}$ and also for set $L_{c,x}$ as a whole. In this paper, we refer to the latter as the generated interpretation audio, x_{int} . For certain classes, it may also be meaningful to listen to each individual component, x_k . As discussed earlier under NMF basics, estimating time domain signals from spectral patterns and their activations typically involves a soft–masking and inverse STFT procedure. We detail this step with appropriate equations in Algorithm 2.

Algorithm 2 Audio interpretation generation

```

1: Input: log-magnitude spectrogram  $\mathbf{X}$ , input phase  $\mathbf{P}_x$  components  $\mathbf{W} = \{\mathbf{w}_1, \dots, \mathbf{w}_K\}$ , time activations
    $\mathbf{H}_{\mathcal{I}}(x) = [\mathbf{h}_1^T(x), \dots, \mathbf{h}_K^T(x)]^T$ , set of selected components  $L_{c,x} = \{k_1, \dots, k_B\}$ .
2: for all  $k \in L_{c,x}$  do
3:    $\mathbf{X}_k \leftarrow \frac{\mathbf{w}_k \mathbf{h}_k^T(x)^T}{\sum_{l=1}^K \mathbf{w}_l \mathbf{h}_l^T(x)^T} \odot \mathbf{X}$  {// Soft masking}
4:    $x_k = \text{INV}(\mathbf{X}_k, \mathbf{P}_x)$  {// Inverse STFT}
5: end for
6:  $\mathbf{X}_{\text{int}} \leftarrow \sum_{k \in L_{c,x}} \mathbf{X}_k$ 
7:  $x_{\text{int}} = \text{INV}(\mathbf{X}_{\text{int}}, \mathbf{P}_x)$ 
8: Output:  $\{x_{k_1}, \dots, x_{k_B}\}$ ,  $x_{\text{int}}$ 

```

4 Experiments

We experiment with two popular audio event analysis benchmarks, namely ESC-50 (Piczak, 2015) and SONYC-UST (Cartwright et al., 2020). While the former is a multiclass environmental sound classification dataset, the latter appeared for DCASE 2019 and 2020 multi-label urban sound tagging task. In this section, we first discuss metrics and baselines used to evaluate our interpretations. This is followed by various implementation details and dedicated subsections to discuss quantitative and qualitative results on each of the aforementioned datasets.

4.1 Evaluation metrics and baselines

Metrics. We evaluate our interpretations in two ways. First, by evaluating how well it agrees with the classifier’s output. For multi-class classification, this is done by computing fraction of samples where the class predicted by f is among the top- k classes predicted by the interpreter. We refer to this as the *top- k fidelity*.

To compute *fidelity* on multi-label classification tasks, we primarily rely on computing Area Under Precision-Recall Curve (AUPRC) based metrics between the classifier output $f(x)$ and its approximation by interpreter $\Theta(\mathbf{H}_{\mathcal{I}}(x))$. We compute macro-AUPRC, micro-AUPRC. Additionally, we report the maximum micro F1-score over different thresholds for the interpreter’s output.

We also conduct a *faithfulness* evaluation for our interpretations. In general for any interpretability method, *faithfulness* tries to assess if the features identified to be of high relevance are *truly* important in classifier’s prediction (Alvarez-Melis & Jaakkola, 2018). Since a “ground-truth” importance measure for features is rarely available, attribution based methods evaluate faithfulness by performing feature removal (most often by setting feature value to 0) and observing the change in classifier’s output (Alvarez-Melis & Jaakkola, 2018). However, it is hard to conduct such evaluation for non-attribution based *post-hoc* interpretation methods (for *e.g.* concept based) on data modalities like image or audio. This is because simulating feature removal from input is not evident in these cases.

Interestingly, the design of our interpretation module allows us to simulate removal of a set of components from the input. Given any sample x with predicted class c , we remove the set of relevant components $L_{c,x} = \{k : r_{k,c,x} > \tau\}$ by creating a new time domain signal $x_2 = \text{INV}(\mathbf{X}_2, \mathbf{P}_x)$, where $\mathbf{X}_2 = \mathbf{X} - \sum_{l \in L_{c,x}} \mathbf{X}_l$. We define faithfulness of the interpretation to classifier f for sample x with:

$$\text{FF}_x = f(x)_c - f(x_2)_c \quad (6)$$

where $f(x)_c, f(x_2)_c$ denote the output probabilities for class c . For multi-class datasets, we opt for measuring absolute drop in logit value instead of absolute drop in probability. This is because class probabilities are also affected by changes in logit values for other classes. It should be noted that this strategy to simulate removal may introduce artifacts in the input that can affect the classifier’s output unpredictably. Also, interpretations on samples with poor fidelity can lead to negative FF_x . Both of these observations point to the potential instability and outlying values for this metric. Thus, we report the final faithfulness of the system as median of FF_x over test set, denoted by $\text{FF}_{\text{median}}$. A positive value for $\text{FF}_{\text{median}}$ would signify that interpretations generally tend to be faithful to the classifier.

Evaluated systems. We denote our proposed Listen to Interpret (L2I) system, with attention based pooling in Θ by $\text{L2I} + \Theta_{\text{ATT}}$. The most suitable baselines to benchmark its fidelity are *post-hoc* methods that approximate the classifier over input space with a single surrogate model. We select two state-of-the-art systems, FLINT (Parekh et al., 2021) and VIBI (Bang et al., 2021). A variant of our own proposed method, $\text{L2I} + \Theta_{\text{MAX}}$, is also evaluated. Herein, attention is replaced with 1D max-pooling operation. Implementation details of the baselines are discussed in Appendix A.1.4.

Faithfulness benchmarking: As already discussed, it is not possible to measure faithfulness for concept-based *post-hoc* interpretability approaches. While measurement for input attribution based approaches is possible, the interpretations themselves and the feature removal strategies are different, making comparisons with our system significantly less meaningful. We thus compare our faithfulness against a *Random Baseline*, wherein the less-important components, those not present in $L_{c,x}$, are randomly removed. To compare fairly, we remove the same number of components that are present in $L_{c,x}$ on average. This would validate that, if the interpreter selects *truly* important components for the classifier’s decision, then randomly removing the less important ones should not cause a drop in the predicted class probability/logit.

We also emphasize at this point that works related to audio interpretability (see Sec. 2.1), are not suitable for comparison on these metrics. Particularly, APNet (Zinemanas et al., 2021) is not designed for *post-hoc* interpretations. AudioLIME (Haunschmid et al., 2020) is not applicable on our tasks as it requires known predefined audio sources. Moreover, SLIME (Mishra et al., 2020) and AudioLIME still rely on LIME (Ribeiro et al., 2016) for interpretations. It is a feature-attribution method that approximates a classifier for *each* sample separately. As discussed before, these characteristics are not suitable for comparison on our metrics.

4.2 Implementation details

Classification network. We interpret a VGG-style convolutional neural network proposed by Kumar et al. (2018). This network was chosen due to its popularity and applicability for various audio scene and event classification tasks. It can process variable length audio and has been pretrained on

| System | Fidelity (in %) | | |
|-----------------------------|-----------------|----------------|----------------|
| | top-1 | top-3 | top-5 |
| L2I + Θ_{ATT} | 65.7 \pm 2.8 | 81.8 \pm 2.2 | 88.2 \pm 1.7 |
| L2I + Θ_{MAX} | 73.3 \pm 2.3 | 87.8 \pm 1.8 | 92.7 \pm 1.2 |
| FLINT | 73.5 \pm 2.3 | 89.1 \pm 0.4 | 93.4 \pm 0.9 |
| VIBI | 27.7 \pm 2.3 | 45.4 \pm 2.2 | 53.0 \pm 1.8 |

Table 1: Top- k fidelity results on ESC-50 environmental sound classification test dataset.

AudioSet (Gemmeke et al., 2017), a large-scale weakly labeled dataset for sound events. It takes as input a log-mel spectrogram. The architecture broadly consists of six convolutional blocks and one convolutional layer with pooling for final prediction. Since it is pre-trained on AudioSet, we first fine-tune it on each of our datasets, fix it, and then learn the interpretation module. Fine-tuning details can be found in Appendix A.1.2

Audio processing parameters. For both the tasks, we perform same audio pre-processing steps. All audio files are sampled at 44.1kHz. STFT is computed with a 1024-pt FFT and 512 sample hop size, which corresponds to about 23ms window size and 11.5ms hop. The log-mel spectrogram is extracted using 128 mel-bands.

Hyperparameters and training. The hidden layers input to the interpreter module are selected from the convolutional block outputs. As is often the case with CNNs, the latter layers are expected to capture higher-order features. We thus select the last three convolutional block outputs as input to the network Ψ . We do not employ any data augmentation for any task. For ESC-50, we pre-learn the dictionary \mathbf{W} with $K = 100$ components and train for 35 epochs on each cross-validation fold. For SONYC-UST, we learn \mathbf{W} with $K = 80$ components and train for 21 epochs. Please refer to Appendix A.1.3 regarding a note on selection of K . We fix $\alpha = 10, \beta = 0.8$ for both datasets. All the training was performed on a single NVIDIA-K80 GPU.

4.3 Experiments on ESC-50

Dataset. ESC-50 (Piczak, 2015) is a popular benchmark for environmental sound classification task. It is a multi-class dataset that contains 2000 audio recordings of 50 different environmental sounds. The classes are broadly arranged in five categories namely, animals, natural soundscapes/water sounds, human/non-speech sounds, interior/domestic sounds, exterior/urban noises. Each clip is five-seconds long and has been extracted from publicly available recordings on the freesound.org project. The dataset is prearranged into 5 folds.

Classifier performance. The classifier achieves an accuracy of $82.5 \pm 1.9\%$ over the 5 folds, higher than the average human accuracy of 81.3% on ESC-50.

Quantitative results. Mean and standard deviation of top- k fidelity is calculated over the 5 folds. We show these results in Table 1 for $k = 1, 3, 5$. Among the four systems, VIBI performs the worst in terms of fidelity. This is very likely because it treats the classifier as a black-box, while the other three systems access its hidden representations. This strongly indicates that accessing hidden layers can be beneficial for fidelity of interpreters. FLINT achieves the highest fidelity, very closely followed by L2I + Θ_{MAX} and then L2I + Θ_{ATT} . This experiment serves as a sanity check for our system, that while achieving fidelity performance comparable to state-of-the-art, we hold the advantage of providing listenable interpretations in terms of pre-learnt spectral patterns.

In Table 2, we report median faithfulness $\text{FF}_{\text{median}}$ (absolute drop in logit value) on fold-1 for our primary system L2I + Θ_{ATT} at different thresholds τ . Smaller τ corresponds to higher $|L_{c,x}|$, which denotes the number of components being used for generating interpretations. Thus, for Random Baseline, we report $\text{FF}_{\text{median}}$ at the lowest threshold $\tau = 0.3$, to ensure removal of maximal number of components. To recall the definition of Random Baseline, please refer to Sec. 4.1. $\text{FF}_{\text{median}}$ for L2I + Θ_{ATT} is positive for all thresholds. It is also significantly higher than the Random Baseline, indicating faithfulness of interpretations.

Noise experiment: an interpretability illustration. We qualitatively illustrate that the interpretations are capable of extracting the object of interest and are useful for an end-user to understand the classifier’s prediction. To do so, we generate interpretations after corrupting the

| System | Threshold τ | FF _{median} |
|----------------------|------------------|----------------------|
| L2I + Θ_{ATT} | $\tau = 0.9$ | 0.21 |
| | $\tau = 0.7$ | 0.42 |
| | $\tau = 0.5$ | 0.89 |
| | $\tau = 0.3$ | 1.29 |
| Random Baseline | $\tau = 0.3$ | 0.00 |

Table 2: Faithfulness results (absolute drop in logit value) on ESC-50 test data for different thresholds, τ . We report FF_{median} for proposed L2I + Θ_{ATT} and the Random Baseline.

testing data for fold-1 with white noise at 0dB SNR (signal-to-noise ratio). Some samples for which classifier’s predicted class is in the top-5 classes of interpreter output, are shared on our companion website.¹

4.4 Experiments on SONYC-UST

In this section, we discuss experiments carried out on the urban sound tagging task from the well known Detection and Classification of Acoustic Scenes and Events (DCASE) challenge 2019 & 2020 edition.

Dataset. The DCASE task used a very challenging real-world dataset called SONYC-UST (Cartwright et al., 2019). It contains audio collected from multiple sensors placed in the New York City to monitor noise pollution. It consists of eight coarse-level and 20 fine-level labels. We opt for the coarse-level labeling task that involves multi-label classification into: ‘engine’, ‘machinery-impact’, ‘non-machinery-impact’, ‘powered-saw’, ‘alert-signals’, ‘music’, ‘human-voice’, ‘dog’.

The dataset consists of 13500 training samples and 664 test samples. It suffers from class imbalance, which we mitigate through class-wise weighting of the loss function. Furthermore, while the testing data has been annotated by experts, each training data point has been labeled by three volunteers. We use minority voting to obtain the final ground-truth labels for training (Cartwright et al., 2019). This task is highly challenging for several reasons: (i) since it is real-world audio, the samples contain a very high level of background noise, (ii) the audio sources corresponding to the classes are often weak in intensity, as they are not necessarily close to the sensors, (iii) some classes may also be highly localized in time and more challenging to detect, (iv) lastly, noisy audio also makes it difficult to annotate, leading to labeling noise. This is especially true for training data that was labeled by volunteers.

Classifier performance. Our fine-tuned classifier achieves a macro-AUPRC (official metric for DCASE 2020 challenge) of 0.601. This is higher than the DCASE baseline performance of 0.510 and comparable to the best performing system macro-AUPRC of 0.649 (Arnault & Riche, 2020). Note that it is obtained without use of data augmentation or additional strategies to improve the classifier performance.

Quantitative results. In Table 3, we report the macro-AUPRC, micro-AUPRC and max-F1 for the interpreter output w.r.t classifier. For fairness, we ignore the class ‘non-machinery impact’ from all class-wise evaluations involved in fidelity (*i.e.* macro-AUPRC) or faithfulness. This is because the classifier predicts only one sample in test set with positive label for this class, causing AUPRC scores to vary widely for different interpreters.

VIBI has the worst performance on all three metrics for this dataset as well. In contrast to ESC-50, here the best performing system is L2I + Θ_{ATT} followed by L2I + Θ_{MAX} , and FLINT performing worse than both. We suspect that our proposed L2I systems are better at handling noisy audio. In that, our NMF-styled decoder contains certain components that model noise and do not affect interpretations. In contrast, the attributes in FLINT are completely learnt and lack such well-defined structure. The fidelity results on ESC-50 and SONYC-UST jointly demonstrate that our interpreter can generate high-fidelity *post-hoc* interpretations, comparable to state-of-the-art methods. Moreover, its design is flexible w.r.t different pooling functions.

¹ <https://listen2interpret.000webhostapp.com/>

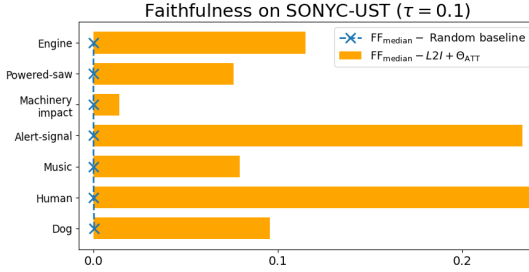


Fig. 2: Faithfulness (absolute drop in probability value) results for SONYC-UST arranged class-wise for threshold, $\tau = 0.1$

| System | Fidelity | | |
|----------------------|-------------|-------------|--------|
| | macro-AUPRC | micro-AUPRC | max-F1 |
| L2I + Θ_{ATT} | 0.900 | 0.914 | 0.847 |
| L2I + Θ_{MAX} | 0.864 | 0.912 | 0.840 |
| FLINT | 0.807 | 0.898 | 0.811 |
| VIBI | 0.608 | 0.575 | 0.549 |

Table 3: Fidelity results on SONYC-UST multi-label urban sound tagging task. We report AUPRC-based metrics and max F1 score for the interpreter w.r.t classifier’s output.

The results for class-wise faithfulness are illustrated in Fig. 2. We show FF_{median} (absolute drop in probability) for our system and the Random Baseline. The results indicate that, for most classes, interpretations can be considered faithful, with a significantly positive median compared to random baseline results, which are very close to 0.

Qualitative observations. Qualitatively, we observe good interpretations for classes ‘alert-signal’, ‘dog’ and ‘music’. For them, the background noise is significantly suppressed and the interpretations mainly focus on the object of interest. Interpretations for class ‘human’ are also able to suppress noise to a certain extent and focus on parts of human voices. However, for this class, we found presence of some signal from other audio sources too. For the remaining classes, namely ‘Engine’, ‘Powered-saw’ and ‘Machinery-impact’ the quality of the interpretation is more sample dependent. This is due to their acoustic similarity with the background noise. We provide some example interpretations for SONYC-UST on our companion website.¹

5 Conclusion

To sum up, we have presented a system for post-hoc interpretation of networks that process audio. We posit that generating interpretations in terms of high-level audio objects and making them listenable are important attributes to aid understanding. Novel usage of NMF within our interpreter helps us satisfy both the aforementioned requirements for understandability. Our original loss function formulation enables linking a classifier’s decision to importance values over pre-learnt NMF spectral dictionary through an intermediate encoding. We perform extensive evaluation over popular audio event analysis datasets. SONYC-UST is particularly challenging due to collection in realistic conditions. We also present first-of-its-kind faithfulness evaluation for our non-attribution based method.

Modular design of our system calls for further experimenting with decoder and other block architectures. We hope our work facilitates future research into designing modality-specific interpreters that aid understanding.

Bibliography

Alvarez-Melis, D. and Jaakkola, T. Towards robust interpretability with self-explaining neural networks. In *Advances in Neural Information Processing Systems (NeurIPS)*, pp. 7775–7784, 2018.

Arnault, A. and Riche, N. CRNNs for urban sound tagging with spatiotemporal context. Technical report, DCASE2020 Challenge, October 2020.

Badeau, R. and Virtanen, T. Nonnegative matrix factorization. *Audio Source Separation and Speech Enhancement*, pp. 131–160, 2018.

Bang, S., Xie, P., Lee, H., Wu, W., and Xing, E. Explaining a black-box by using a deep variational information bottleneck approach. In *Proceedings of the AAAI Conference on Artificial Intelligence*, volume 35, pp. 11396–11404, 2021.

Becker, S., Ackermann, M., Lapuschkin, S., Müller, K.-R., and Samek, W. Interpreting and explaining deep neural networks for classification of audio signals. *arXiv preprint arXiv:1807.03418*, 2018.

Bisot, V., Serizel, R., Essid, S., and Richard, G. Feature learning with matrix factorization applied to acoustic scene classification. *IEEE/ACM Transactions on Audio, Speech, and Language Processing*, 25(6):1216–1229, 2017.

Cartwright, M., Mendez, A. E. M., Cramer, J., Lostanlen, V., Dove, G., Wu, H.-H., Salamon, J., Nov, O., and Bello, J. SONYC urban sound tagging (SONYC-UST): A multilabel dataset from an urban acoustic sensor network. In *Proceedings of the Workshop on Detection and Classification of Acoustic Scenes and Events (DCASE)*, pp. 35–39, October 2019.

Cartwright, M., Cramer, J., Mendez, A. E. M., Wang, Y., Wu, H.-H., Lostanlen, V., Fuentes, M., Dove, G., Mydlarz, C., Salamon, J., et al. Sonyc-ust-v2: An urban sound tagging dataset with spatiotemporal context. *arXiv preprint arXiv:2009.05188*, 2020.

Chowdhury, S., Praher, V., and Widmer, G. Tracing back music emotion predictions to sound sources and intuitive perceptual qualities. *arXiv preprint arXiv:2106.07787*, 2021.

Févotte, C., Vincent, E., and Ozerov, A. Single-channel audio source separation with nmf: divergences, constraints and algorithms. *Audio Source Separation*, pp. 1–24, 2018.

Gao, R., Feris, R., and Grauman, K. Learning to separate object sounds by watching unlabeled video. In *Proceedings of the European Conference on Computer Vision (ECCV)*, pp. 35–53, 2018.

Gemmeke, J. F., Ellis, D. P., Freedman, D., Jansen, A., Lawrence, W., Moore, R. C., Plakal, M., and Ritter, M. Audio set: An ontology and human-labeled dataset for audio events. In *2017 IEEE International Conference on Acoustics, Speech and Signal Processing (ICASSP)*, pp. 776–780. IEEE, 2017.

Ghorbani, A., Wexler, J., Zou, J. Y., and Kim, B. Towards automatic concept-based explanations. In *Advances in Neural Information Processing Systems (NeurIPS)*, pp. 9277–9286, 2019.

Gilpin, L. H., Bau, D., Yuan, B. Z., Bajwa, A., Specter, M., and Kagal, L. Explaining explanations: An overview of interpretability of machine learning. In *2018 IEEE 5th International Conference on data science and advanced analytics (DSAA)*, pp. 80–89. IEEE, 2018.

Goldstein, J. Auditory nonlinearity. *The Journal of the Acoustical Society of America*, 41(3): 676–699, 1967.

Haunschmid, V., Manilow, E., and Widmer, G. audiolime: Listenable explanations using source separation. *arXiv preprint arXiv:2008.00582*, 2020.

Hendricks, L. A., Akata, Z., Rohrbach, M., Donahue, J., Schiele, B., and Darrell, T. Generating visual explanations. In *European Conference on Computer Vision*, pp. 3–19. Springer, 2016.

Ilse, M., Tomczak, J., and Welling, M. Attention-based deep multiple instance learning. In *International conference on machine learning*, pp. 2127–2136. PMLR, 2018.

Kim, B., Wattenberg, M., Gilmer, J., Cai, C., Wexler, J., Viegas, F., and Sayres, R. Interpretability beyond feature attribution: Quantitative testing with concept activation vectors (tcav). *arXiv preprint arXiv:1711.11279*, 2017.

Kingma, D. P. and Ba, J. Adam: A method for stochastic optimization. *arXiv preprint arXiv:1412.6980*, 2014.

Kumar, A., Khadkevich, M., and Fügen, C. Knowledge transfer from weakly labeled audio using convolutional neural network for sound events and scenes. In *2018 IEEE International Conference on Acoustics, Speech and Signal Processing (ICASSP)*, pp. 326–330. IEEE, 2018.

Le Roux, J., Hershey, J. R., and Weninger, F. Deep nmf for speech separation. In *2015 IEEE International Conference on Acoustics, Speech and Signal Processing (ICASSP)*, pp. 66–70. IEEE, 2015a.

Le Roux, J., Weninger, F. J., and Hershey, J. R. Sparse nmf–half-baked or well done? *Mitsubishi Electric Research Labs (MERL), Cambridge, MA, USA, Tech. Rep.*, no. TR2015-023, 11:13–15, 2015b.

Lee, D. and Seung, H. S. Algorithms for non-negative matrix factorization. In Leen, T., Dietterich, T., and Tresp, V. (eds.), *Advances in Neural Information Processing Systems*, volume 13. MIT Press, 2001. URL <https://proceedings.neurips.cc/paper/2000/file/f9d1152547c0bde01830b7e8bd60024c-Paper.pdf>.

Liberman, A., Cooper, F. S., Shankweiler, D. P., and Studdert-Kennedy, M. Why are speech spectrograms hard to read? *American Annals of the Deaf*, pp. 127–133, 1968.

Lundberg, S. M. and Lee, S.-I. A unified approach to interpreting model predictions. In *Advances in Neural Information Processing Systems*, pp. 4765–4774, 2017.

Mahendran, A. and Vedaldi, A. Visualizing deep convolutional neural networks using natural pre-images. *International Journal of Computer Vision*, 120(3):233–255, 2016.

Mishra, S., Sturm, B. L., and Dixon, S. Local interpretable model-agnostic explanations for music content analysis. In *ISMIR*, pp. 537–543, 2017.

Mishra, S., Benetos, E., Sturm, B. L., and Dixon, S. Reliable local explanations for machine listening. In *2020 International Joint Conference on Neural Networks (IJCNN)*, pp. 1–8. IEEE, 2020.

Montavon, G., Samek, W., and Müller, K.-R. Methods for interpreting and understanding deep neural networks. *Digital Signal Processing*, 73:1–15, 2018.

Parekh, J., Mozharovskyi, P., and d’Alché Buc, F. A framework to learn with interpretation. In *Advances in Neural Information Processing Systems (NeurIPS)*, 2021.

Parekh, S., Ozerov, A., Essid, S., Duong, N. Q., Pérez, P., and Richard, G. Identify, locate and separate: Audio-visual object extraction in large video collections using weak supervision. In *2019 IEEE Workshop on Applications of Signal Processing to Audio and Acoustics (WASPAA)*, pp. 268–272. IEEE, 2019.

Peeters, G. and Richard, G. Deep learning for audio and music, 2021.

Piczak, K. J. Esc: Dataset for environmental sound classification. In *Proceedings of the 23rd ACM international conference on Multimedia*, pp. 1015–1018, 2015.

Ribeiro, M. T., Singh, S., and Guestrin, C. Why should i trust you?: Explaining the predictions of any classifier. In *Proceedings of the 22nd ACM SIGKDD international conference on knowledge discovery and data mining*, pp. 1135–1144. ACM, 2016.

Ribeiro, M. T., Singh, S., and Guestrin, C. Anchors: High-precision model-agnostic explanations. In *Proceedings of the AAAI Conference on Artificial Intelligence*, volume 32, 2018.

Selvaraju, R. R., Cogswell, M., Das, A., Vedantam, R., Parikh, D., and Batra, D. Grad-cam: Visual explanations from deep networks via gradient-based localization. In *Proceedings of the IEEE International Conference on Computer Vision*, pp. 618–626, 2017.

Tan, V. Y. and Févotte, C. Automatic relevance determination in nonnegative matrix factorization with the/spl beta/-divergence. *IEEE Transactions on Pattern Analysis and Machine Intelligence*, 35(7):1592–1605, 2012.

Wisdom, S., Powers, T., Pitton, J., and Atlas, L. Deep recurrent nmf for speech separation by unfolding iterative thresholding. In *2017 IEEE Workshop on Applications of Signal Processing to Audio and Acoustics (WASPAA)*, pp. 254–258. IEEE, 2017.

Won, M., Chun, S., and Serra, X. Toward interpretable music tagging with self-attention. *arXiv preprint arXiv:1906.04972*, 2019.

Yeh, C.-K., Kim, B., Arik, S. O., Li, C.-L., Ravikumar, P., and Pfister, T. On concept-based explanations in deep neural networks. *arXiv preprint arXiv:1910.07969*, 2019.

Zinemanas, P., Rocamora, M., Miron, M., Font, F., and Serra, X. An interpretable deep learning model for automatic sound classification. *Electronics*, 10(7):850, 2021.

A.1 Appendix

A.1.1 Sparse-NMF implementation details

As mentioned in Sec. 3.1, a matrix $\mathbf{X}_{\text{train}}$ is constructed from our training dataset and factorized to pre-learn \mathbf{W} . This is done differently for each dataset due to their specific properties. For ESC-50, $\mathbf{X}_{\text{train}}$ is constructed by concatenating the log-magnitude spectrograms corresponding to each sample in the training data of the cross-validation fold (1600 samples for each fold) and performing joint factorization using Eq. 5.

SONYC-UST however, is an imbalanced multilabel dataset with very strong presence of background noise. As a result, we process it differently. We first learn $\mathbf{W}_{\text{noise}}$, that is, a set of 10 components to model noise using training samples with no positive label. Then, for each class, we randomly select 700 positively-labeled samples from all training data and learn 10 new components (per class) with $\mathbf{W}_{\text{noise}}$ held fixed for noise modeling. All $10 \times 8 = 80$ components are stacked column-wise to build our dictionary \mathbf{W} . While this strategy helps us reduce the number of noise-like components in the final dictionary, it does not completely avoid it.

As done in (Bisot et al., 2017), for computational efficiency, we too average the spectrogram frames over chunks of five. This reduces the size of $\mathbf{X}_{\text{train}}$ and saves memory to allow training over more number of samples.

A.1.2 Classifier f training

The architecture we use for f (Kumar et al., 2018) has been pretrained on AudioSet. For each dataset, we first fine-tune this network and perform post-hoc interpretations for that trained network. Here we discuss the specific training details used to fine-tune the classifier architecture.

Details of the full architecture can be found in the original reference. For fine-tuning, we modify the architecture of prediction layers. Specifically, we remove the F2 conv layer and add a linear layer after final pooling, the output dimensions of which correspond to the number of classes in our datasets.

For both the datasets, we do not use any data augmentation. The ADAM optimizer (Kingma & Ba, 2014) is used to fine-tune f . For ESC-50, we only fine-tune the prediction layers of the network. We train the classifier for 10 epochs on each fold of the dataset with a learning rate of 1×10^{-3} .

On SONYC-UST, we fine-tune all the layers in f , which leads to higher classifier AUPRC metrics. The classifier is trained for 10 epochs. Here we start with a learning rate of 2×10^{-4} and halve it after every 4 epochs.

A.1.3 Choosing number of components K

Choice of number of components, K , also known as order estimation, is typically data and application dependent. It controls the granularity of the discovered audio spectral patterns. Choosing K has also been a long standing problem within the NMF community (Tan & Févotte, 2012). Our choice for this parameter was guided by two main factors: (1) choices made previously in literature for similar pre-learning of \mathbf{W} (Bisot et al., 2017), (2) dataset specific details which include number of classes, samples for each class, variability of recordings etc.

(Bisot et al., 2017) show reasonable acoustic scene classification results with a dictionary size of $K = 128$. We use this as a reference to guide our choice for number of components. It is worth mentioning that acoustic variability of ESC-50 (larger number of classes), prompts us to use a dictionary of larger size.

A.1.4 Baseline implementations details

FLINT: We implemented it with the help of their official implementation available on GitHub.² For each experiment, we fix their number of attributes J equal to the number of our NMF components K . We also choose the same hidden layers for their system as we choose for ours. This baseline is trained for the same number of epochs as us. We use same values for our \mathcal{L}_{NMF} loss weight, α ,

² <https://github.com/jayneelparekh/FLINT>

and their \mathcal{L}_{if} loss weight γ . For the other loss hyperparameters, we use their default values and training strategy.

VIBI: We implemented this using their official repository.³ The key hyperparameters that we set are the input chunk size and their parameter K , the number of chunks to use for interpretation. We use a larger chunk size than in their experiments to limit the number of chunks. On ESC-50, we use a chunk size of 32×43 , and on SONYC-UST, a chunk size of 32×86 . This yields 40 chunks for each input on both the datasets. We varied the K from 5 to 20, and report the results with best fidelity. The system was trained for 100 epochs on ESC-50 and 30 epochs on SONYC-UST

³ <https://github.com/SeojinBang/VIBI>